JOURNAL OF THE ROYAL SOCIETY Interface

rsif.royalsocietypublishing.org

Research

Cite this article: Ghriallais RN, McNamara L, Bruzzi M. 2013 Comparison of *in vitro* human endothelial cell response to self-expanding stent deployment in a straight and curved peripheral artery simulator. J R Soc Interface 10: 20120965.
http://dx.doi.org/10.1098/rsif.2012.0965

Received: 23 November 2012
Accepted: 4 January 2013

Subject Areas:
bioengineering, biomedical engineering, biomechanics

Keywords:
peripheral artery, stent, endothelial cell, *in vitro*, bioreactor, haemodynamic force

Author for correspondence:
Ríona Ní Ghriallais
e-mail: r.nighriallais1@nuigalway.ie

Royal Society Publishing
Informing the science of the future

Comparison of *in vitro* human endothelial cell response to self-expanding stent deployment in a straight and curved peripheral artery simulator

Ríona Ní Ghriallais[1,2], Laoise McNamara[1,2] and Mark Bruzzi[1,2]

[1]Department of Mechanical and Biomedical Engineering, and [2]National Centre for Biomedical Engineering Science, National University of Ireland, Galway, Ireland

Haemodynamic forces have a synergistic effect on endothelial cell (EC) morphology, proliferation, differentiation and biochemical expression profiles. Alterations to haemodynamic force levels have been observed at curved regions and bifurcations of arteries but also around struts of stented arteries, and are also known to be associated with various vascular pathologies. Therefore, curvature in combination with stenting might create a pro-atherosclerotic environment compared with stenting in a straight vessel, but this has never been investigated. The goal of this study was to compare EC morphology, proliferation and differentiation within *in vitro* models of curved stented peripheral vessel models with those of straight and unstented vessels. These models were generated using both static conditions and also subjected to 24 h of stimulation in a peripheral artery bioreactor. Medical-grade silicone tubes were seeded with human umbilical vein endothelial cells to produce pseudovessels that were then stented and subjected to 24 h of physiological levels of pulsatile pressure, radial distention and shear stress. Changes in cell number, orientation and nitric oxide (NO) production were assessed in straight, curved, non-stented and stented pseudovessels. We report that curved pseudovessels lead to higher EC numbers with random orientation and lower NO production per cell compared with straight pseudovessels after 24 h of biomechanical stimulation. Both stented curved and stented straight pseudovessels had lower NO production per cell than corresponding unstented pseudovessels. However, in contrast to straight stented pseudovessels, curved stented pseudovessels had fewer viable cells. The results of this study show, for the first time, that the response of the vascular endothelium is dependent on both curvature and stenting combined, and highlight the necessity for future investigations of the effects of curvature in combination with stenting to fully understand effects on the endothelial layer.

1. Introduction

Endothelial cells (ECs) on the lining of the arterial wall are continuously subjected to haemodynamic forces of wall shear stress (WSS), radial pressure and tensile hoop strain (THS) from blood flow. These forces regulate numerous biomechanical stimuli and cellular responses that influence blood vessel structure. Haemodynamic forces have been investigated extensively and it is known that combinations of haemodynamic forces have a synergistic effect on EC proliferation, morphology, biochemical expression and gene expression. Furthermore, alterations to haemodynamic forces influence the development of vascular pathologies [1–9]. Numerous experiments have shown active responses of the vasculature to altered haemodynamic forces, including structural remodelling of the vessel [10–17], altered cell morphologies [18–21], proliferation [14,15,22–24], expression of inflammatory genes ICAM-1 and VCAM-1 [25–28] and production of nitric oxide (NO) [17,28–33].

Under normal physiological conditions, EC function ensures a stable haemodynamic force environment by maintaining EC proliferation, apoptosis and production of adhesion molecules, inflammatory mediators, vasodilators and vasoconstrictors at healthy levels. NO, synthesized by endothelial NOS (eNOS), plays a crucial role in the dilation and remodelling of blood vessels to regulate WSS [17,29,31–34].

Studies have also shown that in the presence of physiological WSS levels, ECs display an elongated appearance, aligned in the direction of flow [3]. ECs reorient perpendicular to the direction of pressure-induced THS, and as such the combined effect of WSS and THS holds significant physiological relevance to cell morphology [8,19].

Changes to flow conditions are commonly observed in peripheral arteries such as the femoropopliteal (FP) artery where curvature is consistently varied along artery length as a result of dynamic loading conditions such as knee bending [35,36]. The artery undergoes considerable length changes during knee bending, compensated by curving and tortuosity of the artery, disrupting flow patterns [37]. In a healthy patient, the control of stable physiological haemodynamics, by the regulatory mechanisms of vessel wall remodelling, ensures that disrupted flow patterns do not lead to a pathological state. However, in patients with risk factors for arterial disease (age, smoking, diabetes, hypertension, obesity and high cholesterol [38]) where the regulatory mechanisms of haemodynamic conditions are compromised, the effects of additional curvatures and disturbed flow may result in an increased likelihood for vascular pathologies to develop in the vessel [38,39].

Percutaneous transluminal angioplasty followed by stent placement is the treatment of choice for arterial occlusion (stenosis) owing to the development of plaque on the inner artery wall [40,41]. While stenting allows uncompromised blood flow through the artery, many investigations report that stenting causes a change in the haemodynamic flow environment owing to stagnation and recirculation of blood flow around stent struts [42–47]. As observed in branched and curved regions, this change in haemodynamic flow conditions is coincident with increased EC proliferation, irregular EC morphologies and lower eNOS expression leading to the return of a pathological state inevitably, restenosis of the vessel [14,15,48,49].

Low WSS (± 4 dyne cm^{-2}), found at branching points, curved and stented regions of the vasculature, are a consequence of flow re-circulation, stasis, separation and directional change [39,50–54]. Low WSS has been correlated with regions of diseased states such as atherosclerosis and stenosis in the carotid, coronary and femoral arteries [14,15,48,49]. Analysis of endothelial layers in regions of turbulent, oscillatory and low WSS shows a build-up of subintimal macrophages and lymphocytes, increased platelet aggregation and EC proliferation, irregular EC morphologies and reduced eNOS production [2,13,20,21,23,24,26–28,30,55]. Altered EC morphologies have a random orientation, exhibit decreased elongation and shortened actin stress fibres eventually causing EC loss. EC loss resulting from low WSS is a proposed result of apoptosis of ECs which remains persistent in the absence of normal WSS levels, eventually leading to a highly diminished EC layer [2,12,22]. Therefore, it can be concluded that intimal hyperplasia, fibrous plaque formation and atherosclerosis are due in part to altered flow conditions, which cause haemodynamic forces to change from normal physiological levels.

Previous studies suggest that a strong connection exists between vessel curvature, stenting, disturbed flow, intima thickening and atherosclerosis, with numerous studies having examined the effects of either artery curvature or stenting on haemodynamic forces using computational models, *in vitro* or *in vivo* studies [2,13–15,20,21,23,24,26–28,30,39,48–55]. However, no study has focused on the effects of both artery curvature changes and stenting in combination and, most importantly, independently of each other. We hypothesize that curved stented arteries create a pro-atherosclerotic environment and that different atherosclerotic responses exist in curved, straight stented and curved stented vessels owing to altered haemodynamic forces. Previous studies have shown the potential of *in vitro* systems to deliver *in vivo* haemodynamic forces [44,56]. Their work also showed the potential of such a system to capture the performance and interaction of coronary stents with the endothelial layer following coronary stent deployment.

The objective of this study was to reproduce the peripheral artery haemodynamic environment using an *in vitro* peripheral artery model and apply this model to determine the effects of curvature change and stent placement on the EC monolayer. A novel peripheral artery simulator is developed to model arteries of varying geometries (i.e. varying curvature), based on a previously existing coronary artery simulator capable of delivering *in vivo* haemodynamic forces *in vitro* [57,58]. Straight and curved sections of silicone tubes (fabricated to match the *in vivo* compliance of the FP artery) are seeded with ECs, stented and subjected to haemodynamic flow conditions for 24 h. EC viability, cell number, orientation and NO production are analysed.

2. Materials and methods

2.1. Bioreactor design

The bioreactor used in this study was adapted from a previous bioreactor perfusion system designed to deliver combinational forces of coronary arterial distention, pressure, flow and WSS to pseudovessels—specially fabricated using silicone tubes seeded with a monolayer of ECs [44]. For the study presented here, the existing bioreactor design was augmented to simulate peripheral arterial radial distention, pressure, flow and mean WSS and to incorporate both straight and curved artery configurations. This was achieved by fabricating a specially designed fixture, capable of attaching the pseudovessel into the flow loop in each configuration. The curved configuration imposes a 0.4 cm^{-1} curvature on the pseudovessel. This was defined by taking the radius of the average bend of the FP artery *in vivo*, 0.4 cm^{-1} [35]. The bioreactor system shown in figure 1 is set up inside a Heraeus Heracell-150 incubator. Pulsatile flow was provided by a peristaltic pump (520U, Watson–Marlow Limited) with the flow profile monitored by a non-invasive ultrasonic flow sensor (H9XL, Transonic Systems Inc.) clipped to the outside the system tubing to ensure a pulse frequency of 1 Hz. The pressure in the system was monitored by a pressure transducer (BLPR2, World Precision Instruments Inc.) connected to the flow loop by a Luer connection. The pressure level in the system was controlled by positioning the reservoir to create a pressure head and by means of an adjustable pinch placed on the outside of the system tubing to control the resistance of the flow in the system. In order to monitor the measurements of flow and pressure, a data acquisition system was set up using

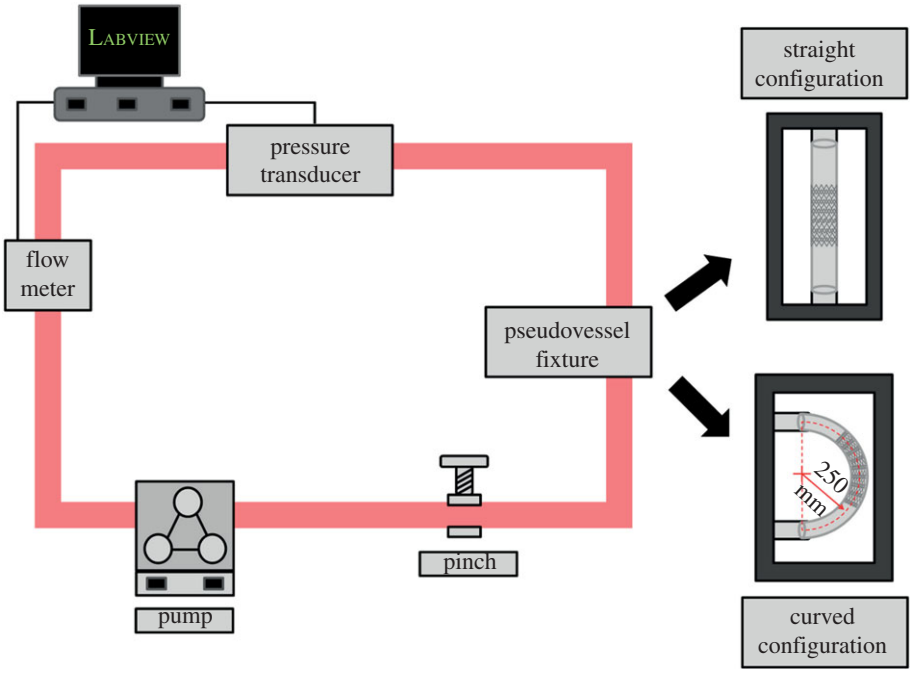

Figure 1. Schematic of bioreactor. (Online version in colour.)

a computer connected to a CompactRIO chassis (NI cRIO-9074, National Instruments) in combination with an input module to read voltage (NI 9215 Input Module). Voltages from the flow probe and pressure transducer were calibrated to ml min^{-1} and mmHg, respectively, using LABVIEW (National Instruments). A LABVIEW program was designed to read the output voltage from the probe and transducer and convert them to ml min^{-1} and mmHg while simultaneously producing live waveforms so that the flow and pressure values could be continuously monitored. The mean WSS applied to the system was calculated from the Hagen–Poiseuille equation [59]:

$$\frac{4\mu Q}{\pi r^3}, \tag{2.1}$$

where μ is the dynamic viscosity of the media (7.21×10^{-4} Pa). A fixture was designed to hold the silicone tube in either a straight or curved configuration during the experiment, attached into the flow loop by flow connectors. The waveform of the flow profile of the bioreactor system is shown in figure 2. The waveform describes the physiological pulsatile flow conditions applied to the pseudovessel with an average flow rate of 240 ml min^{-1}. The average Reynolds number of the flow loop is 391.

2.2. Fabrication of *in vitro* peripheral artery models

Medical-grade silicone (RT-601, Elastosil, Wacker) was moulded into tubes (ID 6 mm, OD 7 mm, length 90 mm) that have comparable material properties to the native FP artery (0.3 MPa elastic modulus, 3.5% radial distention [60–62]). Sterilized silicone tubes were coated with 8 μg ml^{-1} fibronectin (Sigma) and seeded with human umbilical vein endothelial cells (HUVECs) between passages 4 and 6 (PromoCell). HUVECs were seeded at a concentration of 171 500 cells cm^{-2} in EC growth medium (C-22010PromoCell) [44]. Tubes were rotated at slow rotation speed (10 rph) for 48 h (37°C, 5% CO_2). Medium was changed after 24 h. After 48 h of rotation, a short end portion of the tube was cut off and examined to determine a confluent cell layer. The cut section was washed in phosphate-buffered saline (PBS, Sigma) and fixed by immersion in methanol (Sigma) at −21°C for 20 s. Once fixed, the section was stained with haematoxylin (Sigma) for 20 s followed by eosin (Sigma) for 20 s. It was

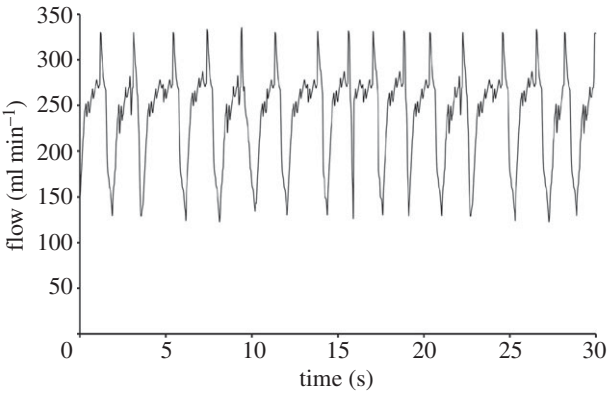

Figure 2. The waveform of the pulsatile flow profile of the bioreactor system recorded using an ultrasonic flow probe.

then longitudinally sectioned with a scalpel and mounted on microscope slides for light microscopy.

2.3. Experimental models

To investigate the effect of curvature on stented peripheral arteries, four experimental models were considered in this study. These included a straight unstented pseudovessel, a curved unstented pseudovessel, a straight stented pseudovessel and a curved stented pseudovessel ($n = 3$ per experimental model).

2.4. Controls

The four models described (straight unstented, curved unstented, straight stented and curved stented) were also investigated in static conditions (no flow) in the bioreactor flow loop as controls ($n = 3$ per control).

2.5. Stent deployment

Once the presence of a confluent cell monolayer was confirmed by haematoxylin and eosin (H&E) staining of a segment of a tube, a nitinol self-expanding stent (7 × 40 mm Cordis S.M.A.R.T. Control nitinol stent system) was deployed into the pseudovessel. The

S.M.A.R.T. stent has regulatory approval for use *in vivo* and therefore has no adverse effect on the ECs of the pseudovessel. The device was received in its original sterile packaging and used in sterile conditions using aseptic techniques. The stent was deployed by means of a stent delivery system in which the stent is crimped and constrained between the inner and outer sheath of a catheter. For stent deployment, the catheter tip is fed through the centre of the pseudovessel and once the stent is positioned correctly, the outer sheath retracted along the inner sheath, allowing the stent to expand to its nominal diameter within the pseudovessel. Following deployment, the inner sheath is retracted from inside the tube. During deployment, care was taken to ensure there was no contact between the delivery system and the EC lining of the tube. The stent was not dragged or repositioned so as not to damage the EC layer. In this way, the innocuousness of the stent deployment is ensured. The stent has a strut profile of 0.1×0.2 mm, and the surface coverage of the stent is calculated as 27.43 per cent of the pseudovessel. Cell viability was measured immediately after stent deployment, using an alamar blue cell viability reagent (Invitrogen). Pseudovessels were washed with PBS (Sigma) and stained with alamar blue (diluted 1 : 10 in cell culture media (C-22010 PromoCell) under a slow rotation speed (10 rph, 37°C, 5% CO_2) for 2 h after which the absorbance of the cell-conditioned alamar blue reagent was measured at 550 and 595 nm using a micro plate reader (Wallac 1420m, Victor). Cell number was quantified by comparing with a standard curve correlating a known cell number with per cent reduction of the alamar blue reagent.

2.6. Biomechanical stimulation

Stented pseudovessels were transferred into the bioreactor flow loop by attachment into the specially designed fixture. Pseudovessels were biomechanically conditioned (pressure 80/120 mmHg, radial distention 5%, average flow of 240 ml min^{-1}, mean WSS 10 dyne cm^{-2}) for 24 h at 37°C, 5 per cent CO_2.

2.7. Cell number

After 24 h of biomechanical conditioning, cell number was measured as previously described using alamar blue cell viability reagent (Invitrogen). Briefly, pseudovessels were removed from the flow loop, washed with PBS (Sigma), stained with alamar blue dye under a slow rotation speed (10 rph, 37°C, 5% CO_2) for 2 h. Absorbance of the cell-conditioned alamar blue reagent was measured and cell quantified using the standard curve correlating a known cell number with per cent reduction of the alamar blue reagent.

2.8. Cell orientation

After 24 h of biomechanical conditioning, the angle of cell orientation was determined. The pseudovessels were washed in PBS (Sigma) and fixed by immersion in methanol (Sigma) at −21°C for 20 s. Once fixed, the tubes were then stained with haematoxylin (Sigma) for 20 s followed by eosin (Sigma) for 20 s. Tubes were longitudinally sectioned with a scalpel so that sections from the entire circumference of the tube could be imaged. Sections were mounted on microscope slides for light microscopy, and images were captured throughout the length of the sections. ImageJ software was used to determine cell orientation by quantifying the orientation of the cells with the longitudinal axis of the tube using the ellipsis method by thresholding the images and using the particle analysis tool to assign best-fit ellipses to each cell [58,63].

2.9. Nitric oxide production

NO production of the cells was monitored during each experiment at 2, 4, 6 and 24 h of biomechanical stimulation. At 2, 4, 6 and 24 h time points, the pseudovessel was removed from the flow loop, washed with PBS (Sigma), filled with cell culture media (C-22010 PromoCell) and incubated for 2 h (37°C, 5% CO_2). Medium was then removed from the tubes, and the tube placed back into the flow loop. Nitrite concentration was quantified from the cell-conditioned media using a Measure-iT high-sensitivity nitrite assay kit according to manufacturer's instructions (Invitrogen).

2.10. Statistical analysis

Results presented here are a representative of three independent experiments for each model and are presented as mean ± s.d. An independent *t*-test was used to determine statistical difference in the fold increase, cell orientation and NO results of the models. A p-value < 0.05 was considered statistically significant. p-Values of significant results are reported.

3. Results

3.1. Cell number

Successful fabrication of pseudovessels followed by self-expanding stent deployment was achieved in the model arteries, confirmed by an alamar blue assay showing viability of cells after seeding and rotation for 48 h. The number of cells at 0 and 24 h in the bioreactor for both static and flow experiments is shown in figure 3*a*. The relative change in cell number from 0 to 24 h is shown in figure 3*b*.

3.1.1. Flow versus no flow

All static condition models show a lower increase in cell number after 24 h compared with their corresponding models subjected to flow conditions (straight unstented, $p = 0.0018$; curved unstented, $p = 0.0005$; straight stented, $p < 0.0001$; curved stented, $p = 0.0005$; figure 3*b*). The highest increase in cell number is seen in the straight stented pseudovessel after addition of flow (1.50-fold increase after 24 h; figure 3*b*). The lowest increase in cell number of the flow models was the straight unstented pseudovessel (1.29-fold increase after 24 h; figure 3*b*).

3.1.2. Straight versus curved

For the unstented models, curved unstented pseudovessels show significantly higher increases in cell number than straight unstented pseudovessels after 24 h of biomechanical flow conditions. (1.29- and 1.41-fold increase for straight unstented and curved unstented models, respectively; $p = 0.0182$; figure 3*b*). Histology of the tubes shows more confluent EC layers in curved unstented tubes versus straight unstented tubes (figure 4). For the stented models, straight stented pseudovessels show significantly higher increases in cell number than curved stented pseudovessels after 24 h of biomechanical flow conditions (1.50- and 1.35-fold increase for straight stented and curved stented models, respectively; $p = 0.0161$; figure 3*b*).

3.1.3. Stented versus unstented

Increase in cell number was significantly higher in the straight stented models in comparison with the straight unstented models after 24 h of biomechanical flow conditions (1.29- and 1.50-fold increase for straight unstented and straight stented models, respectively; $p < 0.0024$; figure 3*b*). The fold

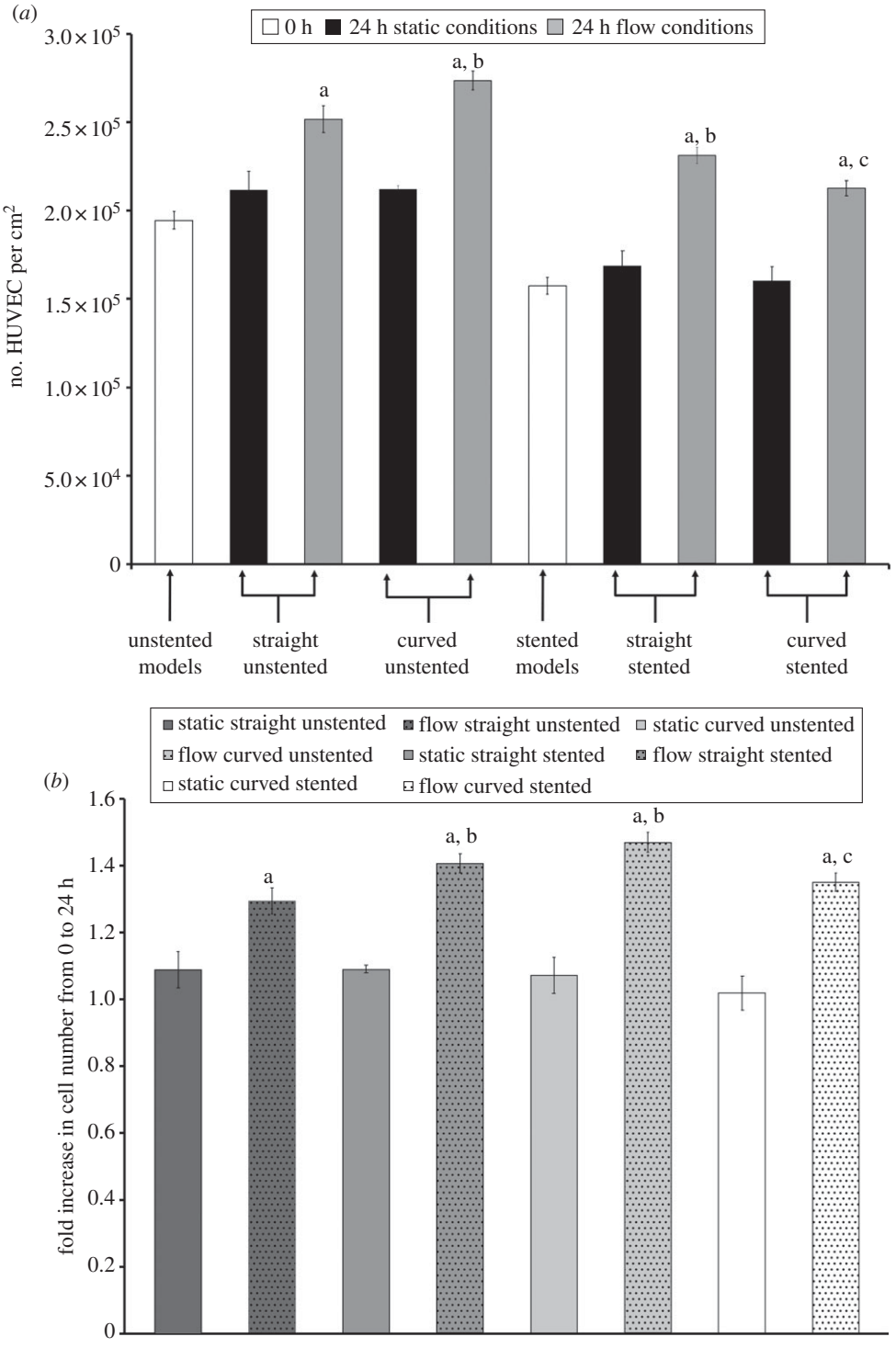

Figure 3. (*a*) Cell number at 0 and 24 h with and without biomechanical flow conditions. $p^a < 0.05$ versus its static control; $p^b < 0.05$ versus straight unstented with flow; $p^c < 0.05$ versus straight stented with flow. (*b*) Relative cell number increase from 0 to 24 h with and without biomechanical flow conditions. $p^a < 0.05$ versus its static control; $p^b < 0.05$ versus straight unstented with flow; $p^c < 0.05$ versus straight stented with flow.

increase in cell number was lower in the curved stented model than the curved unstented model after 24 h of biomechanical flow conditions (1.29- and 1.50-fold increase for curved unstented and curved stented models, respectively; figure 3*b*).

3.2. Cell orientation

3.2.1. Flow versus no flow

Static condition models all showed a random orientation of cells after 24 h (figure 4). Straight and curved unstented pseudovessels had significantly more cells aligned within 10° and 20° of the longitudinal axis of the tube than their static controls (straight unstented 0–10°, $p < 0.0001$; straight unstented 11–20°, $p < 0.0001$; curved unstented 0–10°, $p < 0.0001$; curved unstented 11–20°, $p < 0.0001$). The straight stented pseudovessels had significantly more cells aligned within 0–10° of the longitudinal axis of the tube than its static controls (straight stented 0–10°, $p = 0.0165$; figures 4 and 5).

3.2.2. Unstented pseudovessels

Significantly more cells are seen to align within 0–10° of the longitudinal axis of the tube in the straight unstented pseudovessel compared with the curved unstented pseudovessels

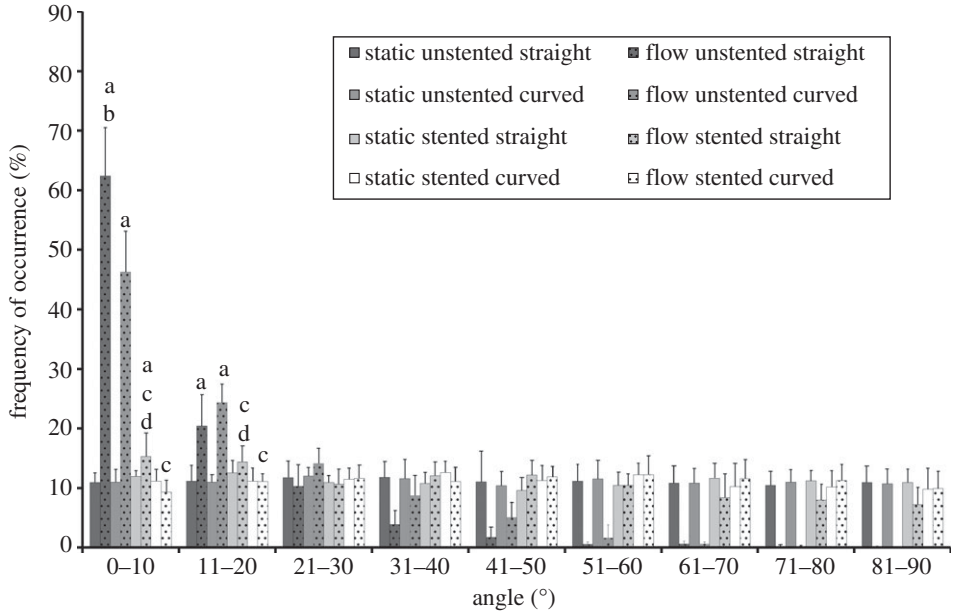

Figure 4. Cell orientation angles and frequency of occurrence for pseudovessels with and without biomechanical flow conditions. $p^a < 0.05$ versus static control; $p^b < 0.05$ versus curved unstented with flow; $p^c < 0.05$ versus corresponding unstented model with flow; $p^d < 0.05$ versus curved stented model.

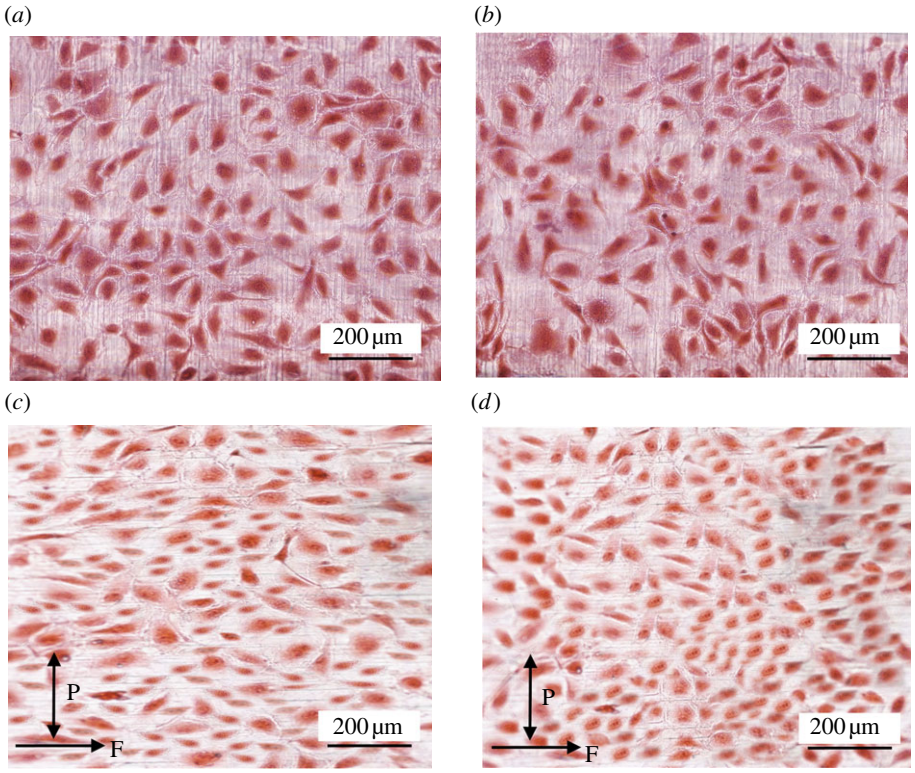

Figure 5. Haematoxylin and eosin-stained unstented pseudovessels after 24 h in the bioreactor. Straight static control pseudovessel (*a*), curved static control pseudovessel (*b*), straight pseudovessel with biomechanical flow conditions (*c*), curved pseudovessel with biomechanical flow conditions (*d*). P and F correspond to pulsatile and flow directions, respectively. (Online version in colour.)

after 24 h of biomechanical stimulation ($p < 0.0001$; figure 4). ECs of the straight unstented pseudovessel are notably more aligned in a particular direction versus the ECs of the curved unstented pseudovessel in histological sections (figure 5*c*,*d*).

3.2.3. Stented pseudovessels

The stented flow models display a significantly less aligned orientation of cells in both straight and curved geometries compared with their corresponding unstented models in the presence of flow (straight stented 0–10°, $p < 0.0001$; straight stented 11–20°, $p = 0.0026$; curved stented 0–10°, $p < 0.0001$; curved stented 11–20°, $p < 0.0001$; figure 4). Significantly less alignment is seen in between stent struts for the curved stented pseudovessel versus the straight stented pseudovessel after 24 h of biomechanical stimulation (0–10°, $p = 0.0001$; 11–20°, $p < 0.0014$; figure 4). In histological sections, it can be seen that the curved stented pseudovessel exhibits slightly less confluent regions of EC growth in between stent struts versus the straight stented pseudovessel, with

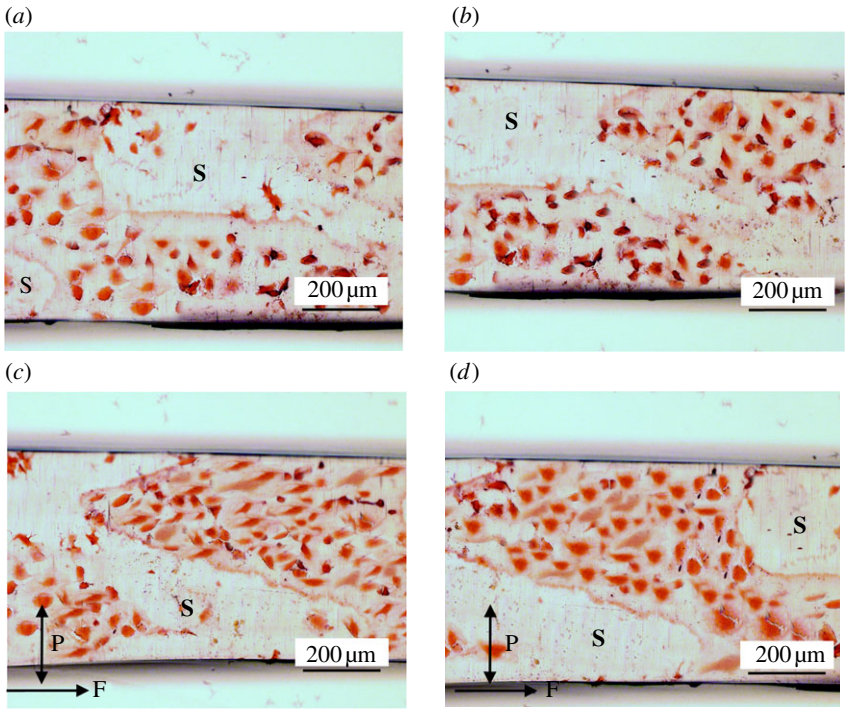

Figure 6. Haematoxylin and eosin-stained stented pseudovessels after 24 h in the bioreactor. Straight static control pseudovessel (*a*), curved static control pseudovessel (*b*), straight pseudovessel with biomechanical flow conditions (*c*), curved pseudovessel with biomechanical flow conditions (*d*). Nitinol stent (S) removed from stented pseudovessels. P and F correspond to pulsatile and flow directions, respectively. (Online version in colour.)

ECs of the curved stented pseudovessel notably less aligned in a particular direction versus ECs of the straight stented pseudovessel (figure 6).

3.3. Nitric oxide production

3.3.1. Flow versus no flow

The static condition models showed low NO production with no statistical difference in NO levels between the different pseudovessels. Addition of biomechanical flow significantly increased NO production in each group (straight unstented, $p < 0.0001$ at 2, 4, 6 and 24 h; curved unstented, $p < 0.0001$ at 2, 4, 6 and 24 h; straight stented, $p < 0.0001$ at 2, 4, 6 and 24 h; curved stented, $p < 0.0001$ at 2, 4, 6 and 24 h; figure 6).

3.3.2. Straight versus curved

Under *in vitro* fluid flow conditions, curved pseudovessels produced significantly less NO than straight pseudovessels in both the unstented and stented case at all time points in the unstented pseudovessels and after 2 h in the stented pseudovessels (curved unstented 2 h, $p = 0.0001$; curved unstented 4 h, $p = 0.0002$; curved unstented 6 h, $p = 0.0025$; curved unstented 24 h, $p < 0.0001$; curved stented 4 h, $p < 0.0001$; curved stented 6 h, $p = 0.0009$; curved stented 24 h, $p < 0.0001$; figure 6).

3.3.3. Stented versus unstented

Under *in vitro* fluid flow conditions, stented pseudovessels produced significantly less NO than unstented pseudovessels in both the straight and curved configuration at all time points (straight stented 2 h, $p = 0.0006$; straight stented 4 h, $p = 0.0005$; straight stented 6 h, $p = 0.0001$; straight stented 24 h, $p < 0.0001$; curved stented 2 h, $p = 0.0021$; curved stented 4 h, $p = 0.0038$; curved stented 6 h, $p < 0.0001$; curved stented 24 h, $p < 0.0001$; figure 6).

4. Discussion

Variations of haemodynamic flow (owing to geometry changes and stenting of the pseudovessels) will alter levels of haemodynamic force (WSS and THS) on the EC lining of the vessel, and it has been shown in this study that this produces cellular responses that can be linked to pathological conditions in vessels. The responses focused on in this study are those of proliferation (by quantifying changes to cell number), orientation per alignment and NO production. This study shows, for the first time, the EC response to combinations of straight, curved, stented and unstented peripheral vessel models subjected to 24 h of stimulation in a peripheral artery bioreactor. After 24 h of biomechanical stimulation we report that, compared with straight pseudovessels, curved pseudovessels show characteristics of a pro-atherosclerotic environment. Specifically, this was indicated by a greater increase in the number of ECs and lower NO production in the curved pseudovessels, with EC orientation in the curved pseudovessels randomly aligned, and not aligned in the direction of flow as seen in straight pseudovessels. Our results showed a reduction in viable ECs immediately after stent deployment in the straight and curved pseudovessels. Furthermore, we report that after 24 h of biomechanical stimulation, curved stented pseudovessels show less viable cells with lower increases in cell number and lower NO production than straight stented pseudovessels, indicating a pro-atherosclerotic environment in the curved stented model.

It has been shown in other studies that ECs found in the regions of disturbed flow and low WSS display a response characteristic of increased proliferation, including the build-up macrophages, lymphocytes and platelets [2,13,20, 21,23,24,26–28,30,55]. Therefore, the altered geometry of the curved pseudovessel and the resulting changes to the flow environment and haemodynamic forces are likely to be responsible for the higher increases in cell number in the

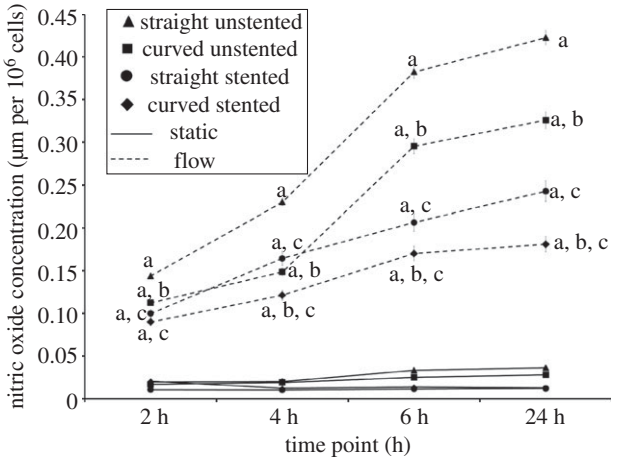

Figure 7. Nitric oxide production for each pseudovessel model at 2, 4, 6 and 24 h in the bioreactor with and without biomechanical flow conditions. $p^a < 0.05$ versus its static control; $p^b < 0.05$ versus corresponding straight pseudovessel with flow; $p^c < 0.05$ versus corresponding unstented pseudovessel with flow.

curved unstented models. In our study, we report for the first time, that lower levels of EC proliferation (lower increase in EC number) are seen in the straight unstented models where normal physiological conditions exist and ECs maintain normal levels of proliferation owing to an environment of stable haemodynamic force. Furthermore, in the absence of haemodynamic forces, in the static condition models, there are little changes to EC number (figure 7).

The reduction in viable ECs seen in the stented pseudovessels post deployment is assumed to be a result of EC denudation during stent placement, which replicates *in vivo* events. It is well known that stent deployment procedures are associated with immediate injury to the EC lining of the vessel wall [64,65]. In this study, it has been shown that increase in EC cell number is lower in the curved pseudovessel than in the straight pseudovessel after stent placement, perhaps owing to the movement of the stent against the pseudovessel wall during attachment to the tube fixture. This friction between the cell-coated tube wall and stent would cause additional denudation of ECs, which does not occur in the straight stented pseudovessel. As the vasculature consists of many curved regions, with curvature changing due to deformation characteristics of the vessel, the *in vitro* model presented here is a good reflection of *in vivo* occurrences. Specifically, it replicates the effects of changing curvature of stented vessels in the superficial femoral artery (SFA) and popliteal arteries that are known to change in curvature due to knee flexion [35,36,66].

In this study, we have also shown that regardless of vessel geometry (straight or curved), the presence of a stent will result in random cell orientation, with regions of aligned ECs populating in close to stent struts. It has been shown in previous studies that the morphological response of ECs is dependent on both WSS and THS and also that the combined effect of WSS and THS holds significant physiological relevance, with cell morphology determined by both haemodynamic forces in combination [16,25]. In the stented models of this study, addition of the stent to the pseudovessel alters its compliance, thereby altering THS. This may be causing the altered morphological EC response seen in the stented pseudovessels, due to changing WSS (around stent struts) and THS (owing to compliance changes) in combination. This study also shows that in a straight stented vessel, there is a greater number of ECs orientating local to stent struts than when the vessel is in a curved configuration. We propose that this is a result of additional changes to flow conditions resulting from the geometry change of the pseudovessel (along with previously mentioned changes to flow conditions owing to the presence of stent struts and compliance of the pseudovessel).

We have shown, for the first time, that the curvature of a stented vessel has an effect on EC proliferation (changes in EC number) post stent deployment. Specifically, it was shown that ECs proliferated less in the curved stented pseudovessel than in the straight stented pseudovessel 24 h after stent deployment in the presence of biomechanical flow conditions. Interestingly, in the absence of flow (in the straight and curved stented pseudovessels in static conditions), no significant difference was seen in the number of viable cells of the straight stented pseudovessel in comparison with the curved stented pseudovessel after 24 h. Therefore, the difference in proliferation rates between the straight and curved stented pseudovessels after 24 h of flow suggests that stenting in combination with artery curvature results in reduced proliferation and viability owing to its haemodynamic force environment. As previously stated, it has been shown that EC response is dependent on both WSS and THS in combination, and it has been suggested that the presence of THS neutralizes the athero-prone effect of low of WSS [16,25]. Studies by both Qiu & Tarbell [16] and Breen *et al*. [25] have reported that THS influences the production of vasoactive agents and cellular proliferation influencing vascular wall remodelling when combined with WSS. In the curved stented models of this study, the addition of the stent to the pseudovessel (which alters pseudovessel compliance and therefore THS) may be a cause of the viability response of the cells in the curved stented pseudovessels in response to changing WSS and THS in combination.

Previous studies have established correlations between altered WSS levels and EC alignment. Steady flow and high WSS levels result in ECs aligning in the direction of flow. Oscillatory/turbulent flow and low WSS levels result in random orientation of ECs [3,4]. Cell orientation results of the static models of this study correlate well with studies that show random alignment of ECs in the absence of flow [3]. Additionally, results of the straight unstented and straight stented pseudovessels compare well with reports by previous researchers that have assessed orientation of cells in straight pseudovessels with and without a stent in the presence of flow [44,56]. We confirm that ECs in these models will align within $0-10^\circ$ of the direction of flow. However, in this study, we show, for the first time, how EC orientation is affected in a curved vessel in the presence of biomechanical flow conditions, both with and without a stent. Specifically, we show that in unstented pseudovessels, ECs are more randomly orientated when the vessel is of a curved configuration. In this study, the curved pseudovessels represent cases of disturbed flow conditions owing to geometry changes, and the resulting EC orientation of these models may therefore be a direct result of disturbed flow conditions.

It has been shown that increased NO production, resulting from high WSS levels inhibits cell proliferation, leading to an overall anti-proliferative effect [33,67]. Therefore, it is possible that high WSS levels, and the resulting production

of NO by ECs in the straight unstented model creates an anti-atherosclerotic environment. In our study, reduced production of NO is found in the curved and stented models and can be explained by changes to haemodynamic forces. In these models, WSS is reduced which has been shown in previous studies to reduce NO production [68,69]. Furthermore, Awolesi *et al.* [70] showed that THS increases EC eNOS expression in bovine aortic ECs. Therefore, the reduced levels of NO production in the stented models of this study could be as a result of lower levels of THS strain. Additionally, as one of the pathways for production of NO is dependent on endothelial receptors on the surface of ECs that form a healthy and complete endothelial layer, allowing binding of ligands essential for NO production [34], the reduced NO level of the stented models may be due to the broken, dysfunctional endothelial layers. Altered levels of NO production are associated with inflammatory and thrombotic responses [34]. Therefore, the curved and stented models of this study display indications of biochemical production that would lead to atherosclerosis and restenosis.

One of the limitations of this experiment is the lack of gene expression analysis. Other studies have examined atherosclerotic responses and restenosis by measuring the expression of inflammatory genes such as ICAM-1, VCAM-1 and E-selectin. However, seen as a complete inflammatory response could only be found through an *in vivo* model with circulating inflammatory cells, an *in vitro* model could not capture an accurate inflammatory response. It was therefore considered sufficient to focus on EC viability, proliferation, orientation and NO production in measuring the response of ECs to curvature and stenting.

As discussed, this study focuses on vascular pathologies influenced by changes in hemodynamic flow conditions. It is important to note that transport and accumulation of macromolecules across the blood vessel wall plays an important role in the physiological regulation of healthy vessels. Therefore, pathological states of the blood vessels such as atherosclerosis are often related to irregular mass transport across the vessel wall [71]. Studies have revealed a correlation between increased permeability to macromolecules (specifically albumin, fibrinogen and low density lipoprotein) and the localization of atherosclerotic plaques [72]. Therefore, mass transport, along with changes to the hemodynamic flow environment, is considered to be a significant factor in vascular pathologies.

Stenting in the FP artery has been associated with high failure rates owing to the challenge faced by the environment of dynamic forces of the SFA and PA, including bending, tension, torsion and compression that leads to failure by stent fracture [73–75]. However, another common cause of stent failure in the FP artery is in-stent restenosis, the recurrence of blockages in the stented region, generally resulting in re-stenting of the artery [76,77]. Restenosis can be considered to be a direct result of the cellular response to changes in flow characteristics which alter the haemodynamic forces of THS and WSS [2,28,30,78]. Therefore, the effects of stenting in combination with artery curvature observed in this study may play a role in in-stent restenosis of FP arteries as stenting in combination with artery curvature dramatically affects flow conditions. In this study, we have examined the effects of both artery curvature and stenting on the endothelial layer *in vitro* independently of each other to elucidate the different result of straight stented and curved stented vessels. The breakdown of these factors will identify the most unfavourable haemodynamic condition of peripheral stented vessels. As FP artery stenting usually involves long stents that extend beyond the lesion, this study highlights that care should be taken when extending the stented portion of the artery to regions of high curvature. Furthermore, the results presented here have important implications for peripheral stent design. A common feature of FP stenting is the 'straightening' of the vessel in the stented portion owing to a mismatch in stiffness between the stented and unstented portion of the vessel immediately adjacent to the stent. This results in increased deformation at the end portions of the stented region and, in turn, geometry changes to the vessel at these locations. Therefore, it can be concluded that stent designs that adversely affect the stiffness of the artery and associated altered vessel configuration post deployment, will undesirably affect cell behaviour to the stented portion and the associated cell responses will ensue.

In conclusion, this study demonstrates that the combination of vessel geometry changes (curvature) and stent deployment, in the presence of haemodynamic flow, results in cell responses associated with pro-atherosclerotic conditions, in-stent restenosis and other arterial diseased states. Furthermore, results presented here highlight the necessity of investigating the effects of curvature in combination with stenting as it has been shown that the response of the vascular endothelium is dependent on both curvature and stenting combined. The use of *in vitro* systems to accurately model the haemodynamic environment of complex arterial geometries such as the FP artery will help to clearly define the effects of altered flow conditions in these regions and the extent of pathophysiological conditions that form as a result.

This work is supported by the Irish Research Council for Science, Engineering and Technology (IRCSET).

References

1. Malek AM, Alper SL, Izumo S. 1999 Hemodynamic shear stress and its role in atherosclerosis. *J. Am. Med. Assoc.* **282**, 2035–2042. (doi:10.1001/jama.282.21.2035)
2. Chiu JJ, Chien S. 2011 Effects of disturbed flow on vascular endothelium: pathophysiological basis and clinical perspectives. *Physiol. Rev.* **91**, 327–387. (doi:10.1152/physrev.00047.2009)
3. Levesque MJ, Nerem RM. 1985 The elongation and orientation of cultured endothelial cells in response to shear stress. *J. Biomech. Eng.* **107**, 341–347. (doi:10.1115/1.3138567)
4. Moore JE, Burki E, Suciu A, Zhao S, Burnier M, Brunner HR, Meister JJ. 1994 A device for subjecting vascular endothelial cells to both fluid shear stress and circumferential cyclic stretch. *Ann. Biomed. Eng.* **22**, 416–422. (doi:10.1007/BF02368248)
5. Barron V, Brougham C, Coghlan K, McLucas E, O'Mahoney D, Stenson-Cox C, McHugh PE. 2007 The effect of physiological cyclic stretch on the cell morphology, cell orientation and protein expression of endothelial cells. *J. Mater. Sci. Mater. Med.* **18**, 1973–1981. (doi:10.1007/s10856-007-3125-3)
6. Wang H, Ip W, Boissy R, Grood ES. 1995 Cell orientation response to cyclically deformed substrates: experimental validation of a cell model.

J. Biomech. **28**, 1543–1552. (doi:10.1016/0021-9290(95)00101-8)

7. Neidlinger-Wilke C, Grood E, Wang JHC, Brand R, Claes L. 2001 Cell alignment is induced by cyclic changes in cell length: studies of cells grown in cyclically stretched substrates. *J. Orthop. Res.* **19**, 286–293. (doi:10.1016/S0736-0266(00)00029-2)
8. Wang JHC, Goldschmidt-Clermont P, Wille J, Yin FCP. 2001 Specificity of endothelial cell reorientation in response to cyclic mechanical stretching. *J. Biomech.* **34**, 1563–1572. (doi:10.1016/S0021-9290(01)00150-6)
9. Dartsch P, Betz E. 1989 Response of cultured endothelial cells to mechanical stimulation. *Basic Res. Cardiol.* **84**, 268–281. (doi:10.1007/BF01907974)
10. Girerd X, London G, Boutouyrie P, Mourad JJ, Safar M, Laurent S. 1996 Remodeling of the radial artery in response to a chronic increase in shear stress. *Hypertension* **27**, 799–803. (doi:10.1161/01.HYP.27.3.799)
11. Langille BL, O'Donnell F. 1986 Reductions in arterial diameter produced by chronic decreases in blood flow are endothelium-dependent. *Science* **231**, 405–407. (doi:10.1126/science.3941904)
12. Bennett MR. 2011 Cell death in cardiovascular disease. *Arterioscl. Thromb. Vas. Biol.* **31**, 2779–2780. (doi:10.1161/ATVBAHA.111.239954)
13. Kamiya A, Bukhari R, Togawa T. 1984 Adaptive regulation of wall shear stress optimizing vascular tree function. *Bull. Math. Biol.* **46**, 127–137. (doi:10.1007/BF02463726)
14. Pedersen E, Kristensen I, Yoganathan A. 1997 Wall shear stress and early atherosclerotic lesions in the abdominal aorta in young adults. *Eur. J. Vasc. Endovasc. Surg.* **13**, 443–451. (doi:10.1016/S1078-5884(97)80171-2)
15. Asakura T, Karino T. 1990 Flow patterns and spatial distribution of atherosclerotic lesions in human coronary arteries. *Circ. Res.* **66**, 1045–1066. (doi:10.1161/01.RES.66.4.1045)
16. Qiu Y, Tarbell JM. 2000 Interaction between wall shear stress and circumferential strain affects endothelial cell biochemical production. *J. Vasc. Res.* **37**, 147–157. (doi:10.1159/000025726)
17. Mattsson EJR, Kohler TR, Vergel SM, Clowes AW. 1997 Increased blood flow induces regression of intimal hyperplasia. *Arterioscler. Thromb. Vas. Biol.* **17**, 2245–2249. (doi:10.1161/01.ATV.17.10.2245)
18. Zhao S, Suciu A, Ziegler T, Moore JE, Bürki E, Meister J-J, Brunner HR. 1995 Synergistic effects of fluid shear stress and cyclic circumferential stretch on vascular endothelial cell morphology and cytoskeleton. *Arterioscl. Thromb. Vasc. Biol.* **15**, 1781–1786. (doi:10.1161/01.atv.15.10.1781)
19. Ives C, Eskin S, McIntire L. 1986 Mechanical effects on endothelial cell morphology: *in vitro* assessment. *In Vitro Cell. Dev. Biol.* **22**, 500–507. (doi:10.1007/bf02621134)
20. Kolpakov V, Polishchuk R, Bannykh S, Rekhter M, Solovjev P, Romanov Y, Tararak E, Antonov A, Mirnov A. 1996 Atherosclerosis-prone branch regions in human aorta: microarchitecture and cell composition of intima. *Atherosclerosis* **122**, 173–189. (doi:10.1016/0021-9150(95)05735-8)
21. Chiu JJ, Wang DL, Chien S, Skalak R, Usami S. 1998 Effects of disturbed flow on endothelial cells. *J. Biomech. Eng.* **120**, 2–8. (doi:10.1115/1.2834303)
22. Cho A, Mitchell L, Koopmans D, Langille BL. 1997 Effects of changes in blood flow rate on cell death and cell proliferation in carotid arteries of immature rabbits. *Circ. Res.* **81**, 328–337. (doi:10.1161/01.RES.81.3.328)
23. Gimbrone MA. 1995 Vascular endothelium: an integrator of pathophysiologic stimuli in atherosclerosis. *Am. J. Cardiol.* **75**, 67B–70B. (doi:10.1016/0002-9149(95)80016-L)
24. Gnasso A, Carallo C, Irace C, Spagnuolo V, De Novara G, Mattioli PL, Pujia A. 1996 Association between intima-media thickness and wall shear stress in common carotid arteries in healthy male subjects. *Circulation* **94**, 3257–3262. (doi:10.1161/01.CIR.94.12.3257)
25. Breen LT, McHugh PE, Murphy BP. 2009 Multi-axial mechanical stimulation of HUVECs demonstrates that combined loading is not equivalent to the superposition of individual wall shear stress and tensile hoop stress components. *J. Biomech. Eng.* **131**, 1880–1892. (doi:10.1115/1.3127248)
26. Nerem R, Alexander R, Chappell D, Medford R, Varner S, Taylor W. 1998 The study of the influence of flow on vascular endothelial biology. *Am. J. Med. Sci.* **316**, 169–175. (doi:10.1097/00000441-199809000-00004)
27. Ishida T, Takahashi M, Corson MA, Berk BC. 1997 Fluid shear stress: mediated signal transduction: how do endothelial cells transduce mechanical force into Biological responses? *Ann. NY Acad. Sci.* **811**, 12–24. (doi:10.1111/j.1749-6632.1997.tb51984.x)
28. Cines DB *et al*. 1998 Endothelial cells in physiology and in the pathophysiology of vascular disorders. *Blood* **91**, 3527–3561.
29. Hayashi T, Yano K, Matsui-Hirai H, Yokoo H, Hattori Y, Iguchi A. 2008 Nitric oxide and endothelial cellular senescence. *Pharmacol. Ther.* **120**, 333–339. (doi:10.1016/j.pharmthera.2008.09.002)
30. Gimbrone MA, Topper JN, Nagel T, Anderson KR, Garcia-CardeÑA G. 2000 Endothelial dysfunction, hemodynamic forces, and atherogenesisa. *Ann. NY Acad. Sci.* **902**, 230–240. (doi:10.1111/j.1749-6632.2000.tb06318.x)
31. Barbato JE, Tzeng E. 2004 Nitric oxide and arterial disease. *J. Vasc. Surg.* **40**, 187–193. (doi:10.1016/j.jvs.2004.03.043)
32. Rudic RD, Shesely EG, Maeda N, Smithies O, Segal SS, Sessa WC. 1998 Direct evidence for the importance of endothelium-derived nitric oxide in vascular remodeling. *J. Clin. Invest.* **101**, 731–736. (doi:10.1172/JCI1699)
33. Förstermann U, Sessa WC. 2012 Nitric oxide synthases: regulation and function. *Eur. Heart J.* **33**, 829–837. (doi:10.1093/eurheartj/ehr304)
34. Klabunde RE. 2004 *Cardiovascular physiology concepts*. Philadelphia, PA: Lippincott Williams & Wilkins.
35. Klein AJ, Chen SJ, Messenger JC, Hansgen AR, Plomondon ME, Carroll JD, Casserly IP. 2009 Quantitative assessment of the conformational change in the femoropopliteal artery with leg movement. *Catheter. Cardiovasc. Interv.* **74**, 787–798. (doi:10.1002/ccd.22124)
36. Cheng CP, Choi G, Herfkens RJ, Taylor CA. 2010 The effect of aging on deformations of the superficial femoral artery resulting from hip and knee flexion: potential clinical implications. *J. Vasc. Interv. Radiol.* **21**, 195–202. (doi:10.1016/j.jvir.2009.08.027)
37. Kröger K, Santosa F, Goyen M. 2004 Biomechanical incompatibility of popliteal stent placement. *J. Endovasc. Ther.* **11**, 686–694. (doi:10.1583/04-127.1)
38. Aboyans V, Criqui MH, Denenberg JO, Knoke JD, Ridker PM, Fronek A. 2006 Risk factors for progression of peripheral arterial disease in large and small vessels. *Circulation* **113**, 2623–2629. (doi:10.1161/circulationha.105.608679)
39. Wood NB, Zhao SZ, Zambanini A, Jackson M, Gedroyc W, Thom SA, Hughes AD, Xu XY. 2006 Curvature and tortuosity of the superficial femoral artery: a possible risk factor for peripheral arterial disease. *J. Appl. Physiol.* **101**, 1412–1418. (doi:10.1152/japplphysiol.00051.2006)
40. David Chua S, MacDonald B, Hashmi M. 2004 Finite element simulation of slotted tube (stent) with the presence of plaque and artery by balloon expansion. *J. Mater. Process. Technol.* **155**, 1772–1779. (doi:10.1016/j.jmatprotec.2004.04.396)
41. Holmes Jr DR *et al*. 1984 Restenosis after percutaneous transluminal coronary angioplasty (PTCA): a report from the PTCA Registry of the National Heart, Lung, and Blood Institute. *Am. J. Cardiol.* **53**, C77–C81. (doi:10.1016/0002-9149(84)90752-5)
42. Frank AO, Walsh PW, Moore JE. 2002 Computational fluid dynamics and stent design. *Artif. Organs* **26**, 614–621. (doi:10.1046/j.1525-1594.2002.07084.x)
43. Duraiswamy N, Schoephoerster RT, Moreno MR, Moore JE. 2007 Stented artery flow patterns and their effects on the artery wall. *Annu. Rev. Fluid Mech.* **39**, 357–382. (doi:10.1146/annurev.fluid.39.050905.110300)
44. Punchard MA, O'Cearbhaill ED, Mackle JN, McHugh PE, Smith TJ, Stenson-Cox C, Barron V. 2009 Evaluation of human endothelial cells post stent deployment in a cardiovascular simulator *in vitro*. *Ann. Biomed. Eng.* **37**, 1322–1330. (doi:10.1007/s10439-009-9701-6)
45. He Y, Duraiswamy N, Frank AO, James E, Moore J. 2005 Blood flow in stented arteries: a parametric comparison of strut design patterns in three dimensions. *J. Biomech. Eng.* **127**, 637–647. (doi:10.1115/1.1934122)
46. Moore JE, Berry JL. 2002 Fluid and solid mechanical implications of vascular stenting. *Ann. Biomed. Eng.* **30**, 498–508. (doi:10.1114/1.1458594)
47. Duraiswamy N, Schoephoerster RT, James E, Moore J. 2009 Comparison of near-wall hemodynamic parameters in stented artery models. *J. Biomech. Eng.* **131**, 061006. (doi:10.1115/1.3118764)

48. Caro C, Fitz-Gerald J, Schroter R. 1971 Atheroma and arterial wall shear observation, correlation and proposal of a shear dependent mass transfer mechanism for atherogenesis. *Proc. R. Soc. Lond. B* **177**, 109–133. (doi:10.1098/rspb.1971.0019)
49. Gnasso A, Irace C, Carallo C, De Franceschi MS, Motti C, Mattioli PL, Pujia A. 1997 *In vivo* association between low wall shear stress and plaque in subjects with asymmetrical carotid atherosclerosis. *Stroke* **28**, 993–998. (doi:10.1161/01.STR.28.5.993)
50. Moore J, Steinman D, Prakash S, Johnston K, Ethier C. 1999 A numerical study of blood flow patterns in anatomically realistic and simplified end-to-side anastomoses. *J. Biomech. Eng.* **121**, 265–272. (doi:10.1115/1.2798319)
51. Deplano V, Bertolotti C, Boiron O. 2001 Numerical simulations of unsteady flows in a stenosed coronary bypass graft. *Med. Biol. Eng. Comput.* **39**, 488–499. (doi:10.1007/BF02345372)
52. Krams R, Bambi G, Guidi F, Helderman F, van der Steen AFW, Tortoli P. 2005 Effect of vessel curvature on Doppler derived velocity profiles and fluid flow. *Ultrasound Med. Biol.* **31**, 663–671. (doi:10.1016/j.ultrdbio.2005.01.011)
53. Prosi M, Perktold K, Ding Z, Friedman MH. 2004 Influence of curvature dynamics on pulsatile coronary artery flow in a realistic bifurcation model. *J. Biomech.* **37**, 1767–1775. (doi:10.1016/j.jbiomech.2004.01.021)
54. Pivkin IV, Richardson PD, Laidlaw DH, Karniadakis GE. 2005 Combined effects of pulsatile flow and dynamic curvature on wall shear stress in a coronary artery bifurcation model. *J. Biomech.* **38**, 1283–1290. (doi:10.1016/j.jbiomech.2004.06.015)
55. Kamiya A, Togawa T. 1980 Adaptive regulation of wall shear stress to flow change in the canine carotid artery. *Am. J. Physiol.* **239**, H14–H21.
56. Cardinal KOH, Bonnema GT, Hofer H, Barton JK, Williams SK. 2006 Tissue-engineered vascular grafts as *in vitro* blood vessel mimics for the evaluation of endothelialization of intravascular devices. *Tissue Eng.* **12**, 3431–3438. (doi:10.1089/ten.2006.12.3431)
57. Punchard MA, Stenson-Cox C, O'Cearbhaill ED, Lyons E, Gundy S, Murphy L, Pandit A, McHugh PE, Barron V. 2007 Endothelial cell response to biomechanical forces under simulated vascular loading conditions. *J. Biomech.* **40**, 3146–3154. (doi:10.1016/j.jbiomech.2007.03.029)
58. O'Cearbhaill ED, Punchard MA, Murphy M, Barry FP, McHugh PE, Barron V. 2008 Response of mesenchymal stem cells to the biomechanical environment of the endothelium on a flexible tubular silicone substrate. *Biomaterials* **29**, 1610–1619. (doi:10.1016/j.biomaterials.2007.11.042)
59. Cheng CP, Parker D, Taylor CA. 2002 Quantification of wall shear stress in large blood vessels using Lagrangian interpolation functions with cine phase-contrast magnetic resonance imaging. *Ann. Biomed. Eng.* **30**, 1020–1032. (doi:10.1114/1.1511239)
60. Benetos A, Laurent S, Hoeks A, Boutouyrie P, Safar M. 1993 Arterial alterations with aging and high blood pressure. A noninvasive study of carotid and femoral arteries. *Arterioscl. Thromb. Vasc. Biol.* **13**, 90–97. (doi:10.1161/01.atv.13.1.90)
61. Bergel D. 1961 The dynamic elastic properties of the arterial wall. *J. Physiol.* **156**, 458–469.
62. Mozersky DJ, Sumnfr DS, Hokanson DE, Strandness Jr DE. 1972 Transcutaneous measurement of the elastic properties of the human femoral artery. *Circulation* **46**, 948–955. (doi:10.1161/01.CIR.46.5.948)
63. Image J. U. S. National Institutes of Health. 1997–2011. See http://imagej.nih.gov/ij.
64. Scott N. 2006 Restenosis following implantation of bare metal coronary stents: pathophysiology and pathways involved in the vascular response to injury. *Adv. Drug Deliv. Rev.* **58**, 358–376. (doi:10.1016/j.addr.2006.01.015)
65. Sullivan TM, Ainsworth SD, Langan EM, Taylor S, Snyder B, Cull D, Youkey J, Laberge M. 2002 Effect of endovascular stent strut geometry on vascular injury, myointimal hyperplasia, and restenosis. *J. Vasc. Surg.* **36**, 143–149. (doi:10.1067/mva.2002.122878)
66. Cheng CP, Wilson NM, Hallett RL, Herfkens RJ, Taylor CA. 2006 *In vivo* MR angiographic quantification of axial and twisting deformations of the superficial femoral artery resulting from maximum hip and knee flexion. *J. Vasc. Interv. Radiol.* **17**, 979–987. (doi:10.1097/01.RVI.0000220367.62137.E8)
67. Golledge J, Turner RJ, Harley SL, Springall DR, Powell JT. 1997 Circumferential deformation and shear stress induce differential responses in saphenous vein endothelium exposed to arterial flow. *J. Clin. Invest.* **99**, 2719–2726. (doi:10.1172/JCI119461)
68. Berkels R, Purol-Schnabel S, Roesen R. 2001 A new method to measure nitrate/nitrite with a NO-sensitive electrode. *J. Appl. Physiol.* **90**, 317–320.
69. Peng X, Recchia FA, Byrne BJ, Wittstein IS, Ziegelstein RC, Kass DA. 2000 *In vitro* system to study realistic pulsatile flow and stretch signaling in cultured vascular cells. *Am. J. Physiol.* **279**, C797–C805.
70. Awolesi MA, Sessa WC, Sumpio BE. 1995 Cyclic strain upregulates nitric oxide synthase in cultured bovine aortic endothelial cells. *J. Clin. Invest.* **96**, 1449–1454. (doi:10.1172/JCI118181)
71. Kennedy JH, Tedgui A. 1995 Normal and pathological aspects of mass transport across the vascular wall. *Cardiovasc. Surg.* **3**, 611–615. (doi:10.1016/0967-2109(96)82858-4)
72. Tarbell JM. 2003 Mass transport in arteries and the localization of atherosclerosis. *Annu. Rev. Biomed. Eng.* **5**, 79–118. (doi:10.1146/annurev.bioeng.5.040202.121529)
73. Scheinert D, Scheinert S, Sax J, Piorkowski C, Bräunlich S, Ulrich M, Boamino G, Schmidt A. 2005 Prevalence and clinical impact of stent fractures after femoropopliteal stenting. *J. Am. Coll. Cardiol.* **45**, 312–315. (doi:10.1016/j.jacc.2004.11.026)
74. Nikanorov A, Smouse HB, Osman K, Bialas M, Shrivastava S, Schwartz LB. 2008 Fracture of self-expanding nitinol stents stressed *in vitro* under simulated intravascular conditions. *J. Vasc. Surg.* **48**, 435–440. (doi:10.1016/j.jvs.2008.02.029)
75. Duda SH *et al*. 2002 Sirolimus-eluting stents for the treatment of obstructive superficial femoral artery disease. *Circulation* **106**, 1505–1509. (doi:10.1161/01.cir.0000029746.10018.36)
76. Cheng SWK, Ting AC, Wong J. 2001 Endovascular stenting of superficial femoral artery stenosis and occlusions: results and risk factor analysis. *Cardiovasc. Surg.* **9**, 133–140. (doi:10.1016/s0967-2109(00)00109-5)
77. Gray BH, Sullivan TM, Childs MB, Young JR, Olin JW. 1997 High incidence of restenosis/reocclusion of stents in the percutaneous treatment of long-segment superficial femoral artery disease after suboptimal angioplasty. *J. Vasc. Surg.* **25**, 74–83. (doi:10.1016/s0741-5214(97)70323-9)
78. Wentzel JJ, Gijsen FJH, Stergiopulos N, Serruys PW, Slager CJ, Krams R. 2003 Shear stress, vascular remodeling and neointimal formation. *J. Biomech.* **36**, 681–688. (doi:10.1016/s0021-9290(02)00446-3)